AN EXAMINATION OF GAS COMPRESSOR STABILITY AND ROTATING STALL

Aziz A. Fozi
Solar Turbines Incorporated
San Diego, California 92138

The principal sources of vibration related reliability problems in high pressure centrifugal gas compressors are the re-excitation of the first critical speed or Resonant Subsynchronous Vibration (RSSV), and the forced vibration due to rotating stall in the vaneless diffusers downstream of the impellers. An example of such field problems is documented in reference 1.

This paper describes the results of a test program at the author's company, initiated in 1983 and completed during 1985, that studied the RSSV threshold and the rotating stall phenomenon in a high pressure gas compressor.

SYMBOLS

Values are given in both SI and English units. The measurements and calculations were made in English units.

Alpha 3   Averaged calculated one-dimensional flow angle into the diffuser measured in degrees from tangential

b3   Inlet width of diffuser

N   Speed

Ncr   Rigid Bearing First Critical Speed

R3   Inlet radius of diffuser

RSSV   Resonant Subsynchronous Vibration or re-excitation of the first critical speed (translatory whirl). Stability threshold means conditions at which the RSSV becomes present.

BACKGROUND

The purpose of this test program was to study subsynchronous vibration problems in an offshore gas compressor installation. The plan was to assemble an identical gas compressor and run it at the same pressure and speed conditions in order to create similar instability mechanisms that could be studied and overcome by hardware modifications at the factory.

AREAS OF STUDY

Tests conducted focused on:

1. Stability threshold and how it is influenced by modifications in balance piston hardware.

2. Presence of rotating stall in parallel-wall vaneless diffusers (as a forcing function) and how the development of rotating stall is influenced by diffuser inlet flow angle (ref. 2).

Justification for focusing the test on the balance piston and vaneless diffusers is provided in this section.

The frequency of the subsynchronous vibration matched the first critical speed of the rotor. This indicated a self-excited mechanism. The compressor was designed to operate at 3,100 kPa ab (450 psia) suction and 12,410 kPa ab (1800 psia) discharge pressure. In practice, the compressor was limited to 11,030 kPa ab (1600 psia). Operation above 11,030 kPa ab (1600 psia) was possible but the subsynchronous vibration would cause bearing damage (clearance increase) within a few days.

On account of its sensitivity to discharge pressure, the cause of this instability was thought to be aerodynamic cross-coupling rather than mechanical, such as the influence of oil seals. In fact, the oil seals were not suspect since the seal oil system was referenced to suction pressure and was not a function of the discharge pressure.

Earlier tests conducted on a similar gas compressor at the author's company in 1974 indicated that stability threshold can be increased by relatively simple modifications to the balance piston flow field. The analytical basis for this work was partially drawn from reference 3. Given this background, the test focused on the balance piston as the major source of excitation and its modification to extend the stability limits.

The next step was to identify the cause of vibration occurring at frequencies lower than the RSSV component (around 65 Hz or about 20% running speed) that had become noticeable during tests. The low frequencies involved indicated an aerodynamic forcing function. It is well known that incipient compressor surge is signaled by occurrence of very low frequency vibration (less than 10 Hz is typical). As a matter of fact, during tests under aerodynamic load such as ASME PTC-10 tests, the proximity to surge is announced by the appearance of these low frequencies. It was thus concluded to search for an aerodynamic forcing function as the cause of such low frequency vibration. Rotating stall in the parallel wall vaneless diffusers was the prime candidate. Figure 1 is a typical test spectrum where all these different frequencies are excited.

The test program was divided into two portions. First, the effect of balance piston flow field on stability was studied. Then, the pressure field at the inlet of the last stage diffuser was monitored for rotating stall.
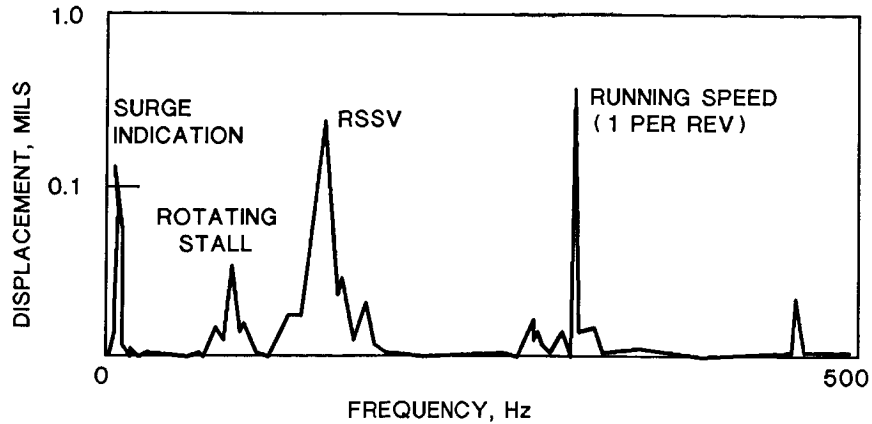
Figure 1. Subsynchronous Vibration Spectrum

TEST PROGRAM DETAILS

Facility

Tests were conducted at the gas compressor closed loop facility of the author's company. This facility in San Diego utilizes a 3200 kW (4300 hp) Centaur gas turbine driver with a step-up gearbox to achieve 24,500 rpm maximum output speed. The gases used were nitrogen or carbon dioxide.

The facility piping is limited to 10,340 kPa gauge (1500 psig) on suction and 31,025 kPa gauge (4500 psig) on discharge. Shell and tube heat exchangers are used to cool the compressed gas.

Compressor

Figure 2 shows a cross section of the gas compressor used for the test. This compressor is capable of 27,580 kPa ab (4000 psia) discharge pressure. The rotor construction features the impellers and suction and discharge stub shafts held together as a monolithic piece by a center tiebolt stretched to provide 311,375 Newtons (70,000 pounds) compressive force. The rotor configuration is straight-through, non-intercooled, with constant impeller hub and shroud labyrinth seal diameter.

The undamped critical speed map (fig. 3) provides rotor-dynamic data. The rigid bearing first critical speed was slightly above 10,000 rpm compared to a typical running speed range of 18,000-23,000 rpm. The rotor weight was 55 kg (122 pounds). Nominal bearing data follow:
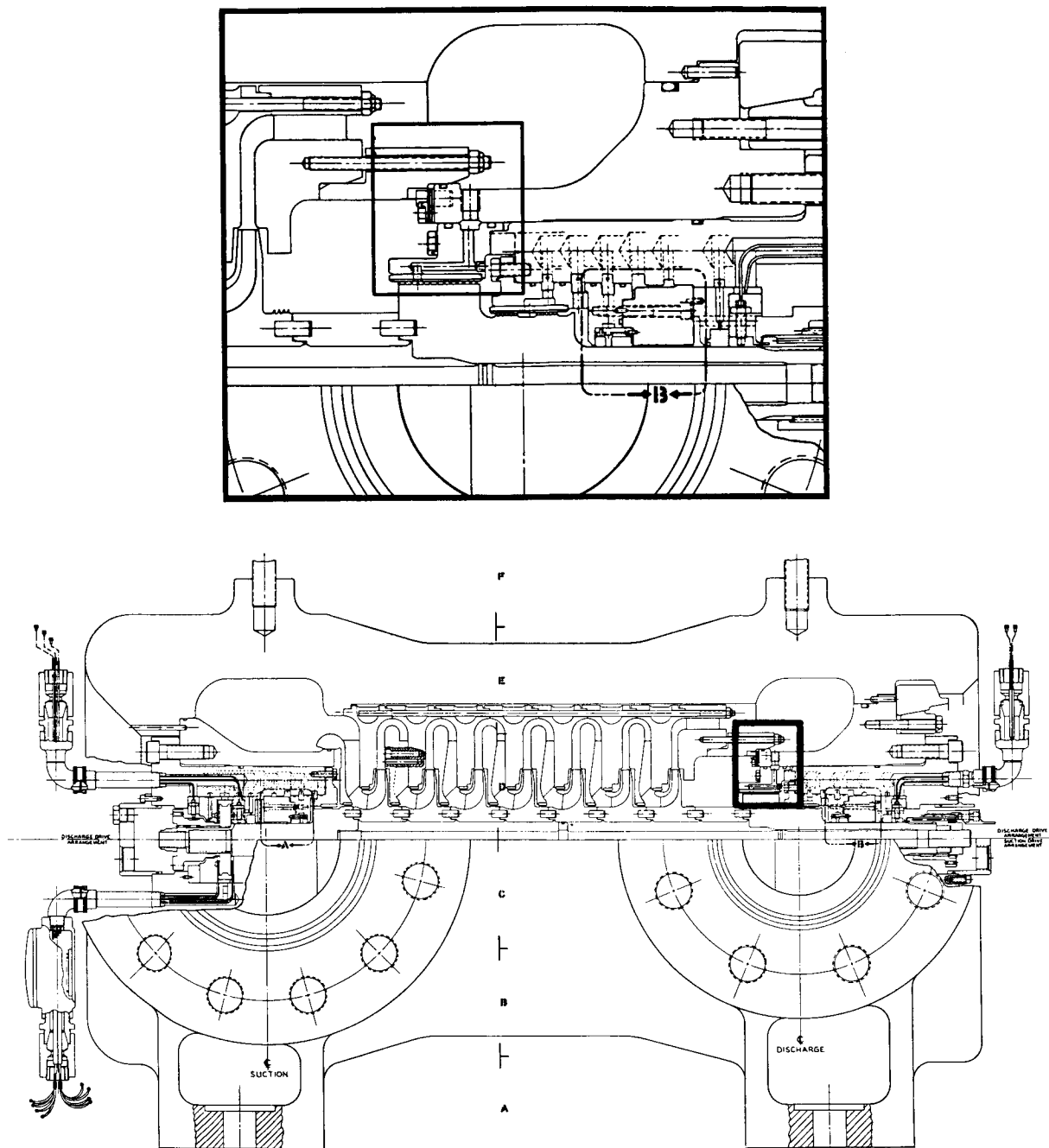
21

Figure 2.   Cross Section of Test Gas Compressor

- Shaft Diameter   44.5 mm (1.75 in.)
- Bearing Clearance Assembled   0.0686 mm (0.0027 in.) – Diametral
- Bearing Preload   0.7
- Pivot Offset   0.6
- Load Position   Between Pivots
- Length/Diameter   0.25
- Number of Pads   5
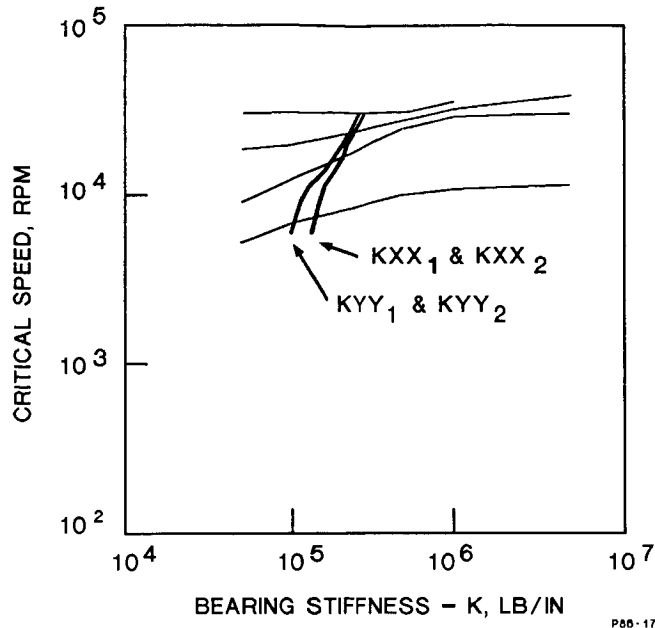- Load on Each Bearing   271 Newtons (61 lb)
- Bearing Span   864 mm (34 in.)

22

Figure 3. Undamped Critical Speed Map

All the labyrinths used were straight-through with the teeth on the rotating elements. The balance piston and impeller shroud seals had a 127 mm (5 in.) diameter. The hub seals had a 94 mm (3.7 in.) diameter. Shaft seals were conventional oil film-type floating rings with anti-rotation pins.

Test Configurations for Stability Threshold

Three balance piston configurations were tested:

- **I - The Baseline Case** - The balance piston flow was taken from the last stage impeller. This is considered the conventional approach (See fig. 4.)

- **II - The 'P2 Inject'** - This configuration is the same as shown in the cross section. The balance piston flow is derived from the discharge cavity and the gas is injected at the third labyrinth tooth. The flow is established because of the dynamic pressure recovery through the last stage diffuser. A portion of injected gas will recirculate back into the last stage diffuser. See figure 5 for detail.

The purpose of 'P2 inject' modification is to eliminate the inlet swirl into the balance piston which is believed to be a strong source of aerodynamic cross coupling forces. Reference 4 is cited here as one of the recent sources of analytical justification for this phenomenon.
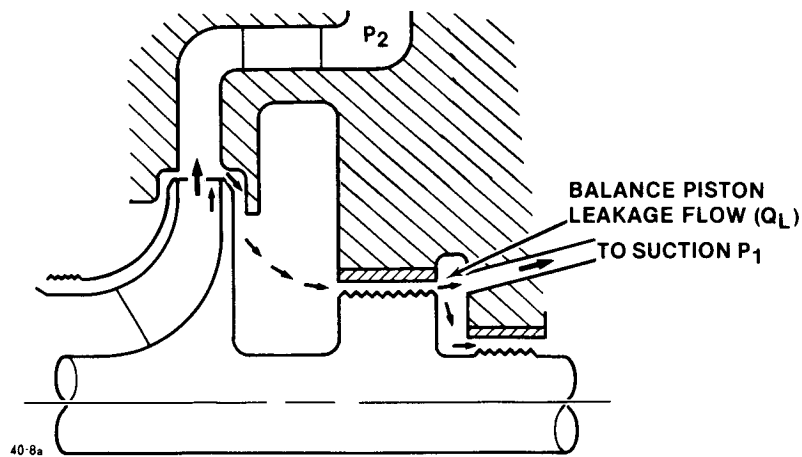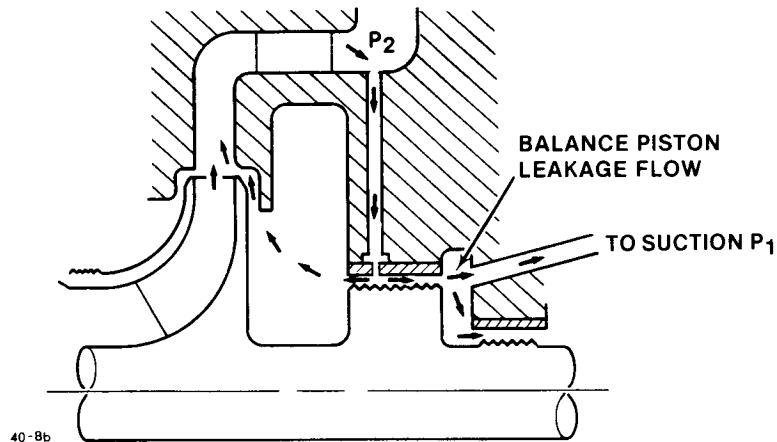
23

Figure 4. Conventional Balance Piston Flow

Figure 5. Balance Piston Flow with P_2-Inject Modification

Some thought was given to direct the 'P2 inject' flow against the rotation to delay the re-establishment of tangential velocity field in the balance piston due to viscous forces. However, the available anti-swirl gas velocity at the injection point appeared to be insufficient to derive any significant results.

III - The 'Hub Seal' - This case was a simplified approach where the balance piston flow is derived from the discharge collector, the last impeller being isolated with a seal at the hub. Thus, the impeller induced swirl is avoided. Figure 6 shows the mechanical details.
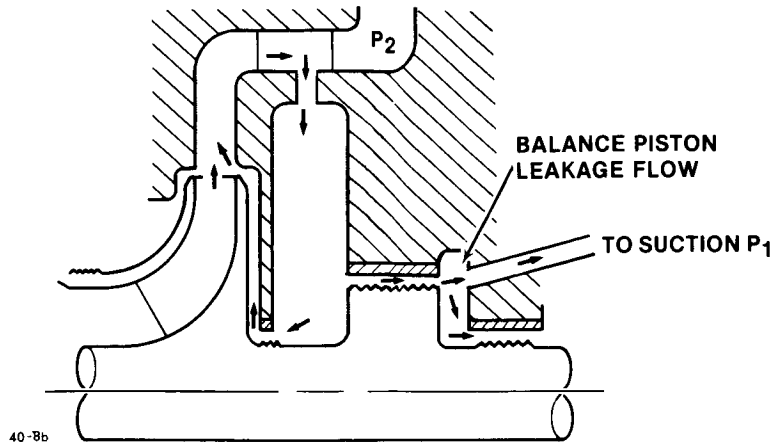
24

Figure 6.   Balance Piston Flow with Hub Seal Modification

Test Configurations for Rotating Stall

Tests were conducted with two diffusers having inlet width-to-radius ratios (b3/R3) of 0.029 and 0.043 respectively, and results were compared to the criteria proposed in refs. 2 and 5. Figure 7 gives dimensional data for the two vaneless diffusers tested. Note that the only difference between the two geometries is in the inlet width (b3).

(b_3) TEST #1 = 0.170 in.
(b_3) TEST #2 = 0.115 in.
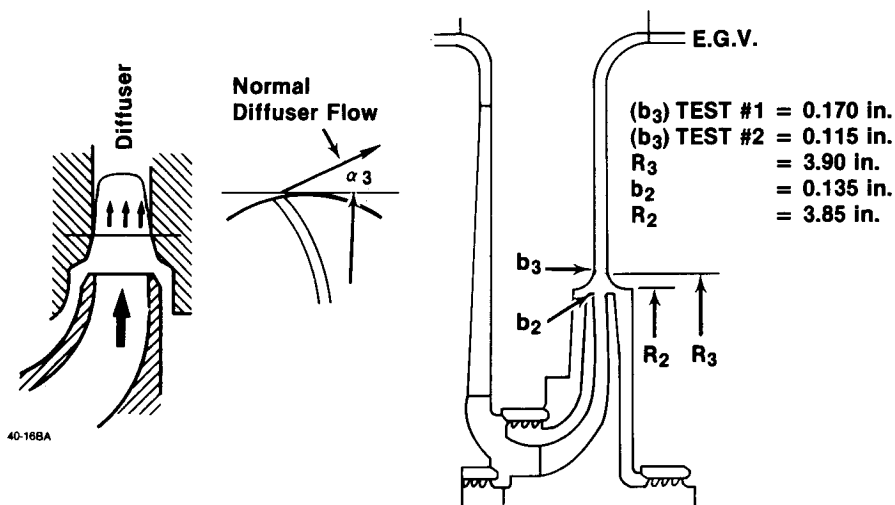R_3 = 3.90 in.
b_2 = 0.135 in.
R_2 = 3.85 in.

Figure 7.   Vaneless Diffuser Geometry

Tests consisted of operating at any constant speed and traversing the compressor operating map from choke towards surge. The diffuser inlet flow angle (Alpha 3) was calculated in real time and displayed. Formation of stall cells was monitored by pressure transducers and data points were recorded as stall cells developed and changed in shape.

25

Instrumentation

The instrumentation used included single- and two-channel FFT spectrum analyzers, a 14-channel tape recorder, and speed tracking balance analyzer. The stall cells were detected by quartz crystal dynamic pressure transducers connected to charge amplifiers displayed on dual trace camera oscilloscopes.

Although one transducer is sufficient to detect the presence of pressure fluctuations (stall), with two transducers the number of stall cells can be calculated based on the observed phase difference between the two signals. See reference 5 for details. Figure 8 shows a detail of the transducer installation.
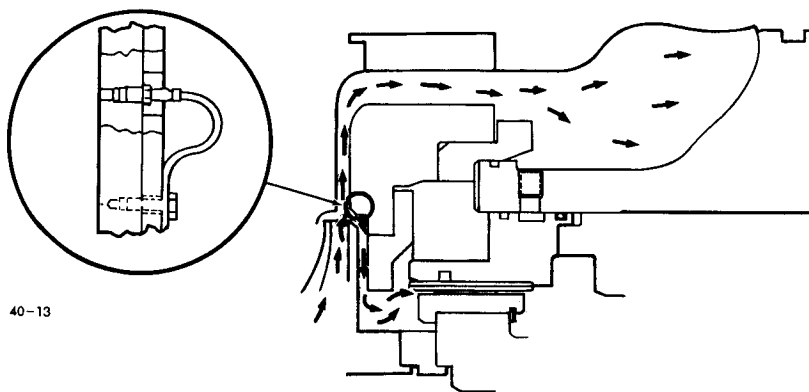

40-13

Figure 8. Pressure Transducer Installation at Diffuser Inlet

Oscilloscope traces presented later are numbered 1 and 2 in the direction of rotation to show phase. The typical amplification factor was a 690 kPa ab (100 psia) dynamic signal per volt, or as indicated on the pictures. The horizontal (milliseconds) and vertical (volts) scales are annotated on these pictures for reference.

The time scale selected favored detection of low frequency signals in the area of 10 to 100 Hz. With this scale, the blade passing frequency at about 6000 Hz is compressed on the oscilloscope trace and is not system noise.

TEST RESULTS

Stability tests concentrated on establishing the threshold at which the RSSV component appeared on the spectrum of shaft vibration at either bearing location. The threshold was established in terms of operating pressure and speed conditions and compared to the criteria proposed in reference 6, namely P2 x (P2-P1), herein referred to as P2 Delta P.

A peak-to-peak shaft vibration amplitude value of 1.27 to 2.54 microns (0.05 to 0.1 mils) was selected as the threshold limit. The results indicated that the P2-inject (Case II) provides better stability than the hub seal (Case III), which itself is an improvement over the baseline (Case I) (figs. 9 and 10).
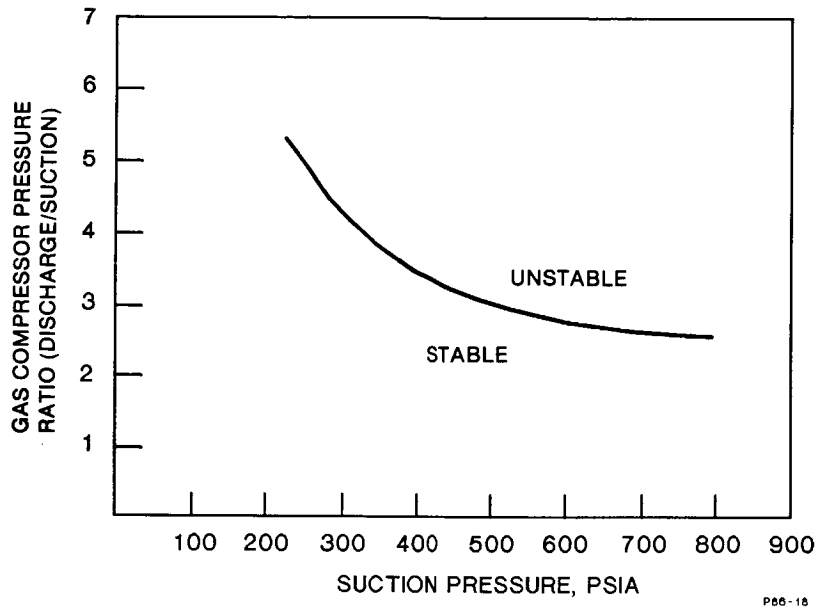

Figure 9.   Stability Threshold of Base Case (Case I)

- **Case I** - The stability line for Case I shows the limit where the RSSV component grows to about 1.27 to 2.54 microns (0.05 to 0.1 mils) peak-to-peak. This line is viewed as analogous to a P2 Delta P range of 1 to 2.5 x E6 (psia square) (fig. 11).

- **Case II** - The P2 inject configuration was stable throughout the tested region. Temperature limits of the facility were reached in every case before any evidence of RSSV was observable. Test facility vibration analyzers were set to high sensitivity to detect the onset of RSSV activity; however, none was detected.

- **Case III** - In figure 10, the hub seal stability limit shows considerable improvement over Case I, comparable to a P2 Delta P range of 4 to 7 x E6. The elimination of impeller swirl at the inlet of the balance piston is thought to be responsible for the improvement.
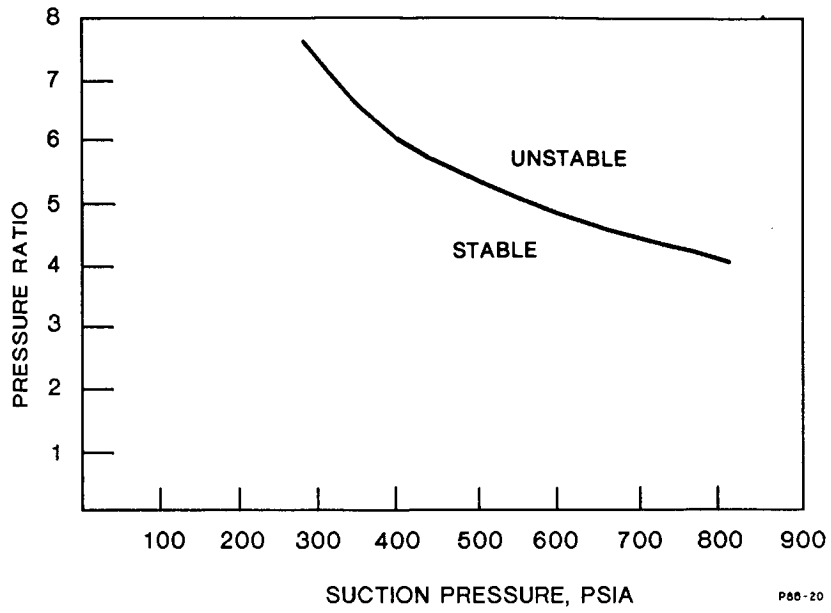
Figure 10. Stability Threshold of Hub Seal Case (Case III)
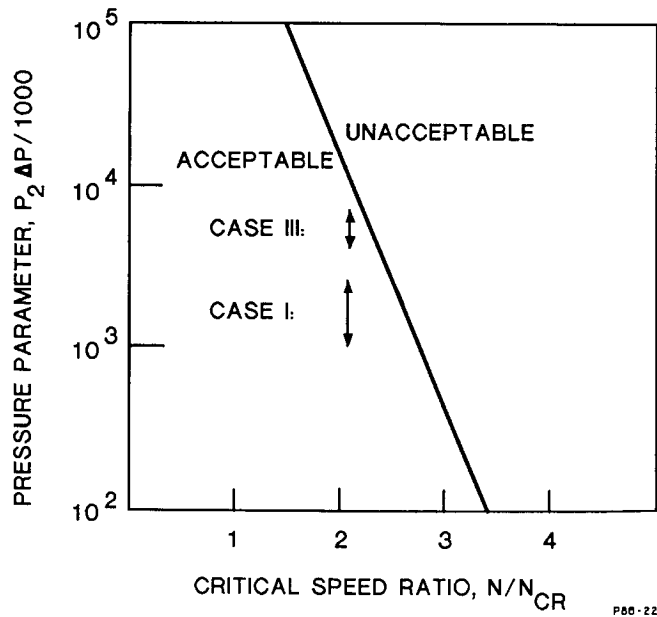

Figure 11. Stability Threshold of Cases I and III

Two observations were made during these tests:

1. The stability threshold for each configuration was defined as a
   function of suction pressure and pressure ratio, and this threshold was
   not dependent on the staging selection or speed. It was found that when
   running on natural gas (S.G. = 0.75) the threshold was the same as when
   running on nitrogen, although at different speeds. Likewise, two
   compressors running on the same gas but staged differently (ten stages
   versus seven stages) gave identical results regardless of speed.
   (Typical variation: 18,000 versus 21,000 rpm.) This was also
   noticeable when examining the threshold lines that were obtained in two
   parts, low suction pressure/high ratio running on carbon dioxide and
   high suction pressure/low ratio running on nitrogen. The threshold was
   a continuous line. This led to the conclusion that the speed was not as
   strong a stability indicator as expected.

2. The RSSV frequency showed dependence on the density of the gas, as
   evidenced implicitly in the following table:

| P1 kPa ab (psia)		Ratio	P2 kPa ab (psia)		Ncr (Hz)	Gas
1,089	(158)	5.8	6,323	(917)	132.5	CO2
1,765	(256)	5.2	9,177	(1,331)	135.0	CO2
2,068	(300)	4.8	9,929	(1,440)	145.0	CO2
3,585	(520)	3.2	11,473	(1,664)	150.0	N2
4,591	(666)	3.0	13,776	(1,998)	152.0	N2
4,964	(720)	2.8	13,900	(2,016)	155.0	N2
5,633	(817)	2.5	14,079	(2,042)	157.5	N2
6,426	(932)	2.2	14,134	(2,050)	160.0	N2

This dependency suggests that labyrinth seals have direct stiffness
terms that tend to restore the deflection of the shaft, thus, raising
the first critical speed. As the density of the compressed gas
increases, the restoring forces become large.
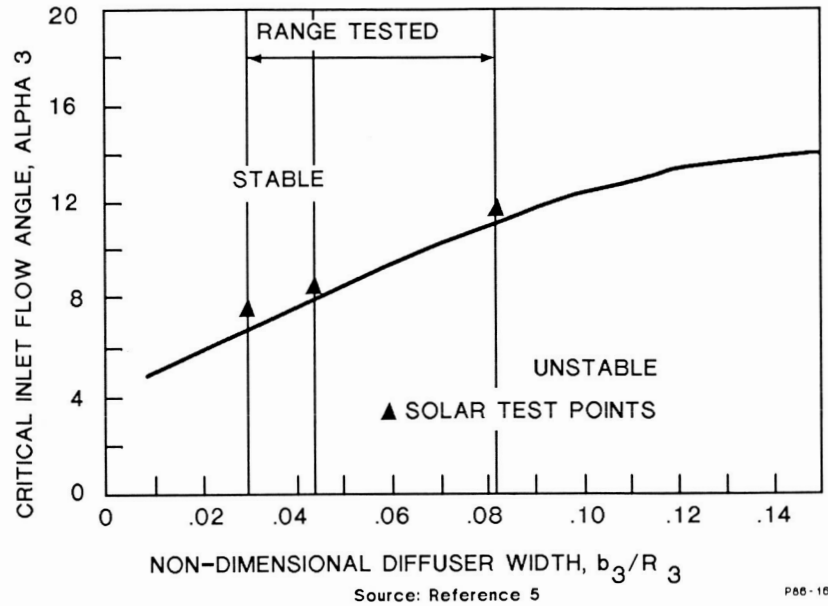
ROTATING STALL

Test Results

The tests showed that the low frequency vibrations on the shaft were
indeed induced by rotating stall. Figure 12 shows a case where one stall cell
at 65 Hz was observed. The transducer separation in this case was 75 degrees.
The 300-Hz signal corresponds to shaft rotation at 18,000 rpm, while the
jitter corresponds to blade passing frequency at 18 times running speed.

The test verified the criterion for the onset of rotating stall as being
the b3/R3 ratio versus the diffuser gas inlet angle (Alpha 3), as described in
references 2 and 5. See figure 13.
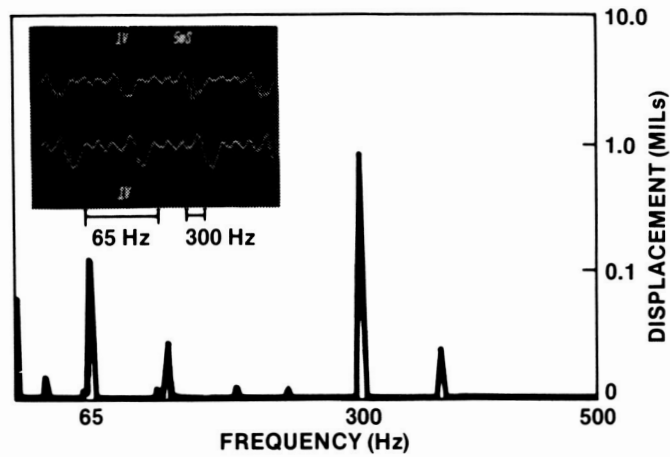
Figure 12.   Shaft Vibration Induced by Rotating Stall

Source: Reference 5

Figure 13.   Rotating Stall Criterion, b3/R3 versus Alpha 3

First, the ratio of b3/R3 of 0.043 was tested. Figures 14, 15, and 16 show
the development of rotating stall as the Alpha 3 angle was reduced from 9.2
degrees to 7 and then to 5.6 degrees [P2 is at 5068 kPa ab (735 psia)]. The
threshold value was obtained at 8.25 degrees, corresponding to the
oscilloscope trace in fig. 17. This figure shows the unsteady pressure field
as stall develops and dissipates.

For a diffuser b3/R3 ratio of 0.029, a critical alpha angle of 7.5 degrees
was obtained. The calculation procedure for alpha angles was based on one-
dimensional flow field analysis. The Reynolds number correction was not
considered in view of the small b3/R3 values of these tests.
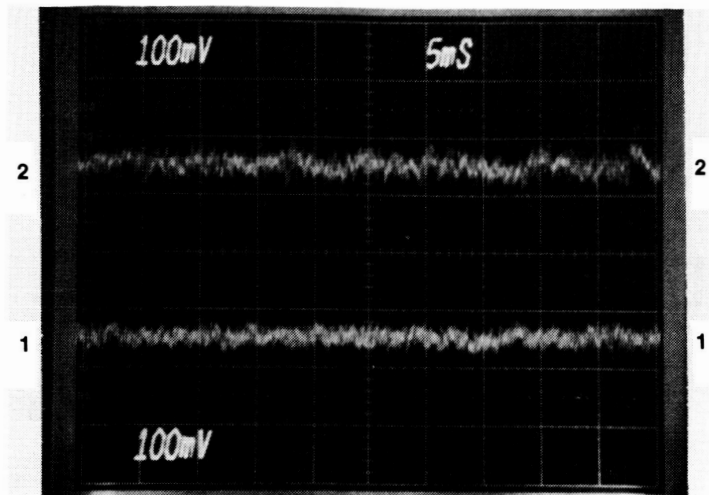
30

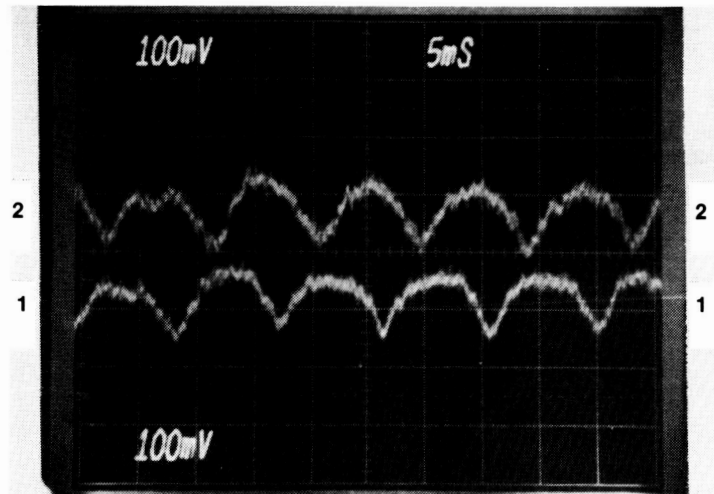Figure 14.   Steady State Pressure Field Prior to Rotating Stall

Figure 15.   Rotating Stall, Two Cells at 56 Hz Rotational Speed

This correlation between low frequency shaft vibration and rotating stall helped interpret results of another investigation. Low frequency vibration was noted when operating a larger frame gas compressor on a particular area of its operating map close to surge. However, careful operation showed that the unit was not at surge and that the amplitude of vibration would actually decrease as flow was lowered to the surge line. (See the performance map in figure 18).

The impeller diameter of this compressor was 305 mm (12 in.) with a b3/R3 ratio of 0.0815. The last stage diffuser flow angles were calculated and drawn on the performance map. The appearance of vibration closely matched the onset of rotating stall predicted at an Alpha 3 of 11.3 degrees. It is interesting to note the high amplitude of vibration at 8 Hz (single stall cell) compared to 16 Hz (two cells) which apparently indicates the cancellation effect of an even number of stall cells.
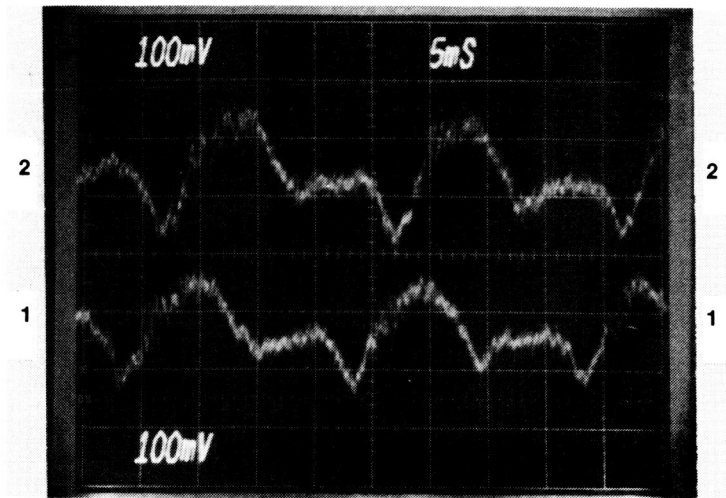
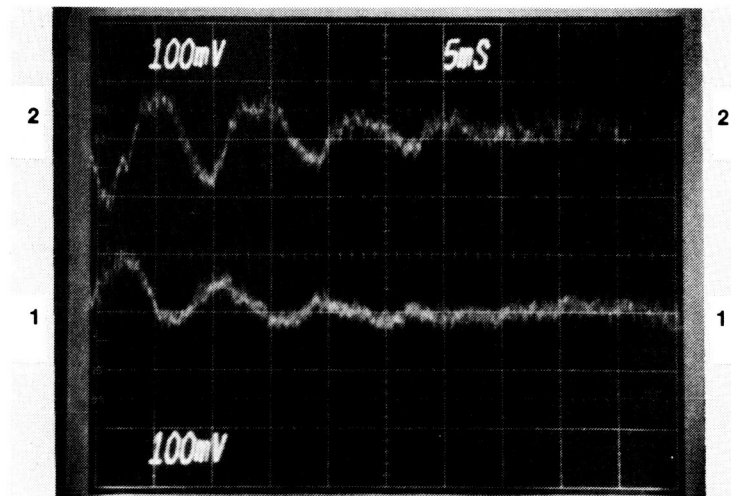Figure 16.   Rotating Stall near Surge

Figure 17.   Threshold Where Stall Cell Appears and Dissipates

CONCLUSION AND COMMENTS

The balance piston is a strong excitation source of instability, and modifications to the inlet swirl have great effect in extending the operating limits of the gas compressor. For any given compressor configuration, the stability limit may be defined in terms of suction pressure versus pressure ratio. The P2 Delta P as a function of the critical speed ratio N/Ncr is a useful index but it over-emphasizes the speed sensitivity. Lastly, the rotating stall criterion of Alpha 3 versus b3/R3 was confirmed.
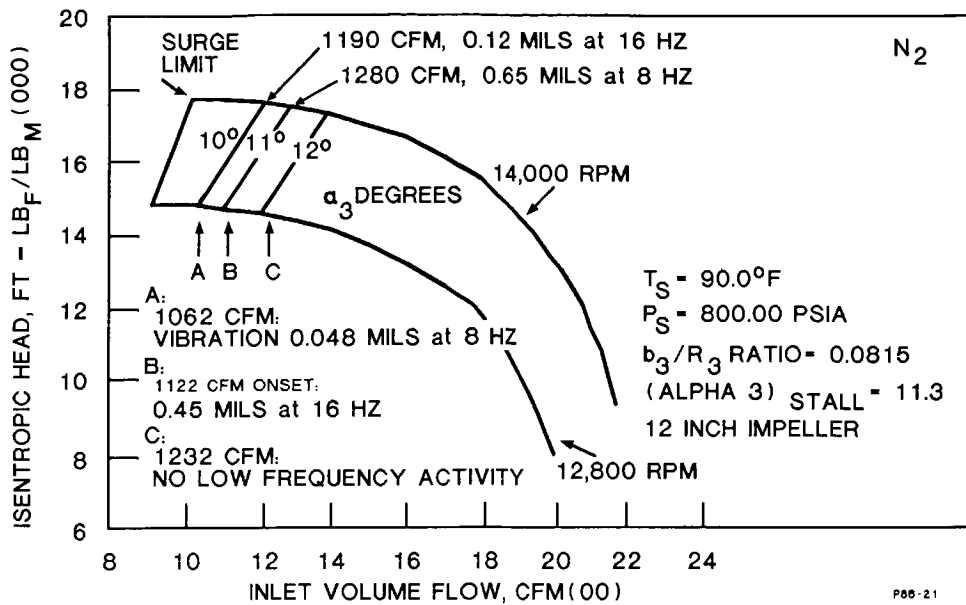
Figure 18. Performance Map with Lines of Constant
Alpha 3 versus Shaft Vibration

REFERENCES

1. Fulton, J.W., "Subsynchronous Vibration of a Multistage Centrifugal
    Compressor Forced by Rotating Stall," Turbomachinery Technology Seminar
    1986, Solar Turbines Incorporated, San Diego, California, February 1986.

2. Kinoshita, Y., Senoo, Y., "Rotating Stall Induced in Vaneless Diffusers of
    Very Low Specific Speed Centrifugal Blowers," ASME 84-GT-203, June 1984.

3. Kostyuk, A.G., "A Theoretical Analysis of the Aerodynamic Forces in the
    Labyrinth Glands of Turbomachines," Moscow Power Institute (MEI), 1972.

4. Childs, D.W., Scharrer, J.K., "An Iwatsubo-Based Solution for Labyrinth
    Seals: Comparison to Experimental Results," ASME 85-GT-136, Texas A&M
    University, College Station, Texas, March 1985.

5. Van Den Braembussche, "Rotating Stall in Vaneless Diffusers of Centrifugal
    Compressors," Technical Note 145, Von Karman Institute, June 1982.

6. Kirk, R.G., Donald, G.H., "Design Criteria for Improved Stability of
    Centrifugal Compressors," ASME Publication "Rotor Dynamic Instability,"
    AMD-Volume 55, June 1983.